Rupture Propagation in a Model of an Earthquake Fault

J. S. Langer and C. Tang
Institute for Theoretical Physics, University of California, Santa Barbara, California 93106
(Received 19 April 1991)

We present analytic and numerical studies of rupture propagation in a one-dimensional model of an earthquake fault. In the case of a fault that is uniformly at its slipping threshold, the propagation speed is determined by a dynamic selection mechanism elsewhere identified as "marginal stability." At any nonzero distance below threshold, however, a solvability principle appears to be applicable. We describe the way in which these two mechanisms turn out to be consistent with each other and comment upon the unusual role of the short-wavelength cutoff.

PACS numbers: 91.30.Mv, 05.70.Ln, 46.30.Nz

Among the interesting problems that have emerged in recent studies [1,2] of the dynamics of a model earthquake fault [3], one of the most challenging is that of predicting the speeds at which ruptures propagate. In the following, we present some analytic and numerical studies that seem to go much of the way toward a solution of this problem. As will be seen, however, this physical situation possesses novel aspects which are, at best, only incompletely explained by the results obtained so far. We believe that these results, as well as the questions that have arisen, may have implications for a broader class of problems pertaining to fracture and shock propagation.

As described in previous publications [1,2], the model of interest here is defined by a partial differential equation of the form

$$\ddot{U}=\frac{\partial^2 U}{\partial s^2}-U-\phi(2a\dot{U}) \tag{1}$$

or, more precisely, by the finite-difference version of this equation:

$$\ddot{U}_j=l^2(U_{j+1}+U_{j-1}-2U_j)-U_j-\phi(2a\dot{U}_j)\,. \tag{2}$$

Here, U_j is the displacement of the elastic medium at position $s=ja$ along the fault, where a is the smallest relevant length scale in the problem, $l=1/a$, and j takes on integer values. The overdots denote differentiation with respect to time t. The dimensionless units in which displacements, position, and time are measured are discussed in detail in Refs. [1] and [2] but will not be of special concern here. Note two small differences between the form of Eqs. (1) and (2) and the way in which they appear in Ref. [2]. Here we have scaled the stiffness length (previously called ξ) to unity because, for present purposes, we want to go immediately to the limit of an infinitely long system; thus, $\xi=1$ and $a=1/l$ are the only relevant length scales. Also, we have set the loading speed (previously called v) to zero because we shall consider only events that occur at some fixed state of stress along the fault.

Apart from the nonlinear friction ϕ, Eq. (1) is a massive wave equation scaled so that both the high-frequency wave speed and the mass are unity. The first term on the right-hand side may be thought of as the force due to tensile strains along the fault, and the second is the force due to the shear strain that has built up in the abutting tectonic plates. The friction ϕ is

$$\phi(2a\dot{U})=\begin{cases}(-\infty,1], & \dot{U}=0\,,\\ 1-2a\dot{U}, & 0<\dot{U}\le 1/2a\,,\\ 0, & \dot{U}>1/2a\,.\end{cases} \tag{3}$$

This, too, is a slightly different version of the stick-slip friction law than the one we used previously; this piecewise linear function is a useful simplification for analytic purposes. The parameter a, which is a measure of the strength of the velocity-weakening instability, is precisely the same as before. We must emphasize that this is a minimal model of an earthquake fault that is missing features that might be relevant to the rupture problem. In particular, it will be interesting to see what happens to rupture propagation in a model where the fault is more realistically coupled to the elastic deformations of the tectonic plates. An important motivation for the present investigation has been to make some progress toward understanding which features of this class of models are relevant to which physical phenomena in realistic systems.

The most dramatic and, apparently, physically realistic feature of this model is that it exhibits two qualitatively different kinds of earthquakelike events: relatively small, localized events with a power-law distribution of magnitudes; and large, delocalized events in which enough energy is released near the epicenter to trigger a propagating rupture, that is, a shock front. A picture of one such delocalized event, typical of those seen in numerical solutions of (2) described in earlier publications, is shown in Fig. 1 as a set of successive configurations $U(s)$ at uniformly spaced times. The bottommost and uppermost curves are, respectively, the initial and final configurations. In this typical situation, the initial configuration is irregular; the regions where U is closest to -1 are the regions where the system is nearest the slipping threshold, and vice versa. The initial motion near the epicenter is complex, but the two shock fronts that subsequently propagate out in opposite directions are remarkably regular. They move at a nearly constant speed, of order unity,

© 1991 The American Physical Society

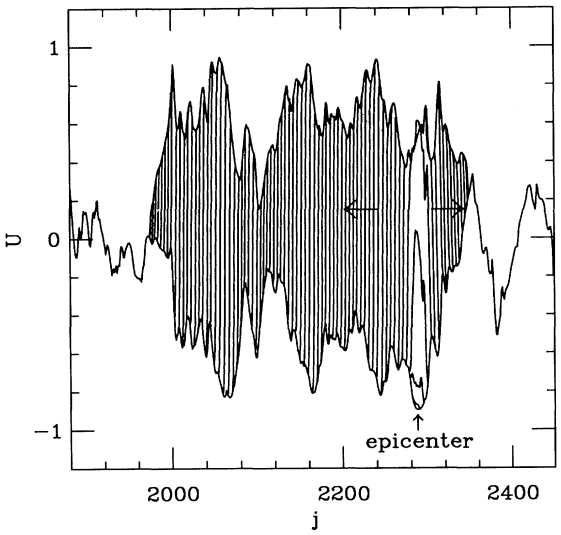

FIG. 1. A set of successive snapshots, at equally spaced times, of configurations U_j as a delocalized event evolves. The nearly vertical lines describe how the displacement at any point j "snaps" quickly from its initial to its final value as the front passes by in the direction shown by the arrows.

somewhat faster in regions where the system is close to threshold and, conversely, more slowly where the system is more tightly stuck. At either end of the event, the shocks die out when they encounter strongly stuck regions of the fault.

In order to study these motions more systematically, it is useful to look at situations in which a rupture is propagating through a system whose displacement is uniformly an amount ϵ away from threshold, that is, $U_j=-1+\epsilon$ for all j. We find by numerical experiments that any shock generated by an initially localized disturbance propagates at a speed c which is a well-defined function of ϵ.

To analyze this motion, we start with the case $\epsilon=0$. This situation looks intriguingly like the one that has been encountered in other contexts in which a dynamically stable state of a system propagates into an unstable state [4–8]. The point of similarity is that the region with $\epsilon=0$, $U=-1$ is unstable, and the region where U has become restuck at some value appreciably greater than -1 is stable in some sense. (An infinitesimal perturbation has no effect because the sticking friction ϕ automatically balances the elastic forces.) There are some important differences, however. In the first place, all of the previously well-studied examples are parabolic differential equations, first order in the time derivative, whereas (1) is a wave equation with an extra unfamiliar kind of nonlinear term ϕ. More importantly, only the finite-difference form, Eq. (2), actually is mathematically well defined if we take literally the multiple-valued friction ϕ given in Eq. (3). As a result, some of the analytic techniques that work for differential equations are not available to us.

In particular, we do not know for sure that this system shares with those studied in Refs. [4–8] the important property that there exists a continuous family of speeds c for which propagating fronts of the form $U(s-ct)$ are exact solutions of the equation of motion. This property usually is demonstrated by mode-counting arguments, which do not work here. Nevertheless, the technique of using the characteristic modes of the linearized equation to study the initially small displacements ahead of the advancing front turns out to be quite productive.

Specifically, we write

$$U_j=-1+u_j(t)\,, \tag{4}$$

where, for j sufficiently far ahead of the front, we may expect u_j to be small enough so that a linear approximation makes sense. For $\dot{u}_j>0$, the linearized version of (2) is

$$\ddot{u}_j=l^2(u_{j+1}+u_{j-1}-2u_j)-u_j+2\alpha\dot{u}_j\,. \tag{5}$$

Solutions of (5) have the form

$$u_j(t)=A(Q)\exp(-Qj+\Omega t)\,, \tag{6}$$

where

$$\Omega(Q)=\alpha\pm[2l^2(\cosh Q-1)+\alpha^2-1]^{1/2}\,. \tag{7}$$

If (6) is to describe the forward region of a front propagating at speed $+c$, and if $\mathrm{Re}Q>0$, then only the plus sign in (7) is relevant, and we must have

$$\Omega(Q)=lcQ\,. \tag{8}$$

This equation has two branches of solutions with real Q for a continuous range of values of c greater than the value c^* at which the line lc^*Q is tangent to the curve $\Omega(Q)$. The "marginal-stability hypothesis" then suggests that c^* is the dynamically selected value of c, and that the corresponding value of Q, say Q^*, describes the selected shape of the front.

More precisely, we expect that any initially localized triggering pulse will generate a front for which Q satisfies the condition that the wave velocity c is the same as the group velocity $c_g(Q)$ (analytically continued to imaginary wave number),

$$c_g(Q)\equiv\frac{1}{l}\frac{\partial\Omega}{\partial Q}=c, \tag{9}$$

which, together with (8), means that $c=c^*$ and $Q=Q^*$. Very crudely, the selected state is the one for which a localized perturbation, moving at $c_g(Q)$, just keeps up with the front. For a more systematic derivation of (9) and a discussion of stability, see Refs. [6] and [7]. A more general and careful analysis has been presented by van Saarloos [8].

To test this dynamic selection hypothesis, we have performed numerical experiments to measure c for $\epsilon=0$ and various values of α and l and have compared these results with the predictions of Eqs. (8) and (9), also obtained

numerically. The results are shown in Fig. 2. The selection mechanism appears to be completely accurate in this limit ($\epsilon=0$). It is also interesting to examine the predictions of (8) and (9) in the continuum limit, $l\gg 1$. To do this, it is necessary only to expand $\cosh Q$ in (7) to order Q^4. The result is

$$Q^* \approx \left(\frac{12a}{l}\right)^{1/3}, \quad c^{*2} \approx 1+\left(\frac{3a}{2l}\right)^{2/3}, \quad l\gg 1. \quad (10)$$

Note that c^* approaches the wave speed (unity) from above as $l\to\infty$. The width of the shock, $\Delta s \cong a/Q^* \approx (12al^2)^{-1/3}$, vanishes in this limit; but the number of finite-difference elements ("blocks" in our previous terminology) contained in the shock front, $\Delta s/a \approx (l/12a)^{1/3}$, diverges. This nontrivial l dependence is a potentially important physical feature of this model [2].

The more difficult problem is to compute the propagation speed c for a system that is initially below the slipping threshold, that is, for $\epsilon>0$. If the analogy to previous work holds true, then there should be only a single value of c, rather than a family of such speeds, for which a propagating solution exists at any positive nonzero ϵ. The mystery is how the system contrives to make such a "solvability" mechanism at $\epsilon>0$ precisely consistent with the dynamic selection mechanism in the limit $\epsilon\to 0$ [9].

The calculation of c at $\epsilon=0$ was simplified by the fact that the exponential tail that extends ahead of the front, although very small, goes smoothly all the way out to infinity. For nonzero ϵ, on the other hand, at any instant of time, there is a well-defined position at which rupture is being initiated. In principle, we must solve the equations of motion accurately near that position, as well as at all other positions, in order to determine the conditions under which a propagating solution exists. In practice, the latter problem is quite difficult. One complication is

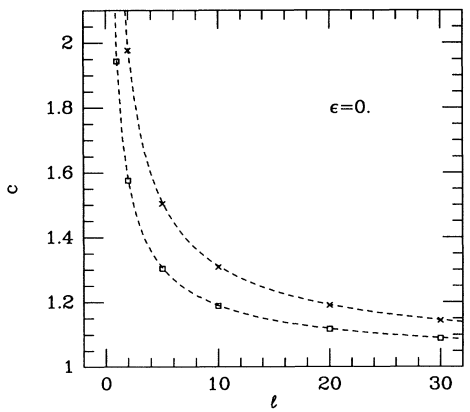

FIG. 2. The speed c of the shock front obtained from numerical solutions of Eq. (2) as a function of l. The crosses are for $a=3$ and the squares for $a=1.5$. The initial configuration is unstable, i.e., $\epsilon=0$. The dashed lines are solutions of Eqs. (8) and (9).

that the selected front may not be stationary in the frame moving at speed c; rather, it may have an oscillating component with frequency c/a. Therefore, we have devised an approximation which, at the expense of introducing one (slightly) adjustable parameter, gives us some extra insight into the nature of the selection mechanism.

Our hypothesis is that, for small ϵ, the front is described accurately by a single exponential mode of the form (6), but that Q must become complex. More precisely, we assume that (6) is valid in some region not too close to the point of initial rupture where many solutions of (5) must be linearly superimposed to match the boundary conditions, but still close enough to that point that the linearization (5) remains valid, that is, $\dot u < 1/2a$. The piecewise linear version of ϕ given in (3) was chosen so as to make the linear equation (5) accurate over as large a range as possible for comparison with numerical analysis. By allowing Q to be complex, we apparently gain just enough degrees of freedom in this one-mode part of the front to be able to construct a smooth solution for one, but no more than one, value of the speed c.

Let $Q=Q_1\pm iQ_2$ be the complex-conjugate pair of solutions of Eq. (8) for $c\lesssim c^*$ and $Q\cong Q^*$, and write, for $j<clt$,

$$u_j(t)\cong A\exp[-Q_1(j-clt)]\cos[Q_2(j-clt)+\delta]+\cdots, \quad (11)$$

where δ is an undetermined phase. The notation "$+\cdots$" in (11) means that the term shown here is part of the linear superposition of solutions of (5) that is needed to match the boundary conditions at the moving point of rupture, $j\cong clt$. In particular, in the quartic approximation for $\cosh Q$ that was used in obtaining (10) for $l\gg 1$ and $\epsilon\approx 0$, there are two other modes of the form $\exp(-Qj)$: a slowly decreasing mode with $Q\approx(2al)^{-1}$, and a rapidly growing mode with $Q\approx -2Q^*$. To make a rough estimate of the amplitude A, we superimpose these modes to fix $u=\epsilon$ and $\dot u=\ddot u=0$ at $j=clt$, and find $A\cos\delta\approx -\epsilon\gamma/(a^2l)^{2/3}$, where $\gamma=[3(12)^{1/3}]^{-1}\cong 0.145$.

Although the term shown explicitly in (11) is small compared to other contributions (which are of order ϵ) near $j=clt$, it becomes the dominant contribution to u_j at the position $j'=clt-\Delta j$ where $2a\dot u=1$ and the slipping friction vanishes. Because $A\cos\delta$ is negative, the cosine in (11) must change sign between j' and j, so that $Q_2\Delta j=\theta\cong\pi$. Thus, the equation determining Δj becomes

$$\dot u_{j'}\cong\frac{\epsilon\gamma Q_1 cl^{1/3}}{a^{4/3}}\exp\left(\theta\frac{Q_1}{Q_2}\right)\cong\frac{1}{2a}, \quad (12)$$

and

$$\frac{Q_1}{Q_2}\cong-\frac{1}{\theta}\ln\left(\frac{2\epsilon\gamma Q_1 cl^{1/3}}{a^{1/3}}\right). \quad (13)$$

Equations (8) and (13) are sufficient to determine

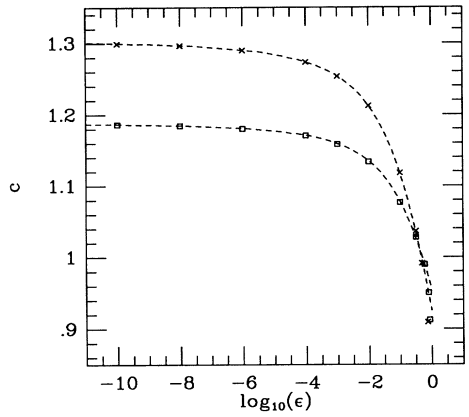

FIG. 3. The speed c of the shock front obtained from the numerical solutions of Eq. (2) as a function of ϵ, for $l=5$ and $\alpha=1.5$ (crosses), and for $l=10$ and $\alpha=1.5$ (squares). The dashed lines are the solutions of Eqs. (8) and (13) with $\theta=\pi$ and $\gamma=0.1$.

$Q=Q_1\pm iQ_2$ and c as functions of ϵ and the ratio α/l.

Our comparisons between the values of c determined by numerical experiments and by solving (8) and (13) are shown in Fig. 3. For reasons that we do not understand, we obtain excellent agreement nearly all the way up to $\epsilon=1$ by choosing $\theta=\pi$ and setting $\gamma=0.1$ instead of 0.145. Remember that it is energetically impossible for rupture to propagate at $\epsilon>1$. Given the fact that all of our analysis is applicable only for small ϵ, and in view of the uncertainty in the value of θ and the crude way in which we have estimated γ, we do not believe that this unexpected agreement is specially significant. The overall pattern of agreement, however, gives us confidence that our basic assumptions are correct. In addition to the data shown in Fig. 3, we have numerically confirmed the prediction that our results, for large enough l, should depend only on the ratio α/l, and not on α or l separately.

Finally, it is useful to write out explicitly the solutions of (8) and (13) in the limit $l\gg 1$:

$$Q_1\approx Q^*\approx\left(\frac{12\alpha}{l}\right)^{1/3},\quad \frac{Q_2}{Q_1}\approx\frac{\theta}{|\ln(2\epsilon/3)|},$$
$$c^2\approx 1+\left(\frac{3\alpha}{2l}\right)^{2/3}\left[1-\frac{\theta^2}{\ln^2(2\epsilon/3)}\right]. \tag{14}$$

The most important feature of these formulas is that the width of the region in which the linear approximation is valid, $\Delta j\approx\theta/Q_2$, diverges logarithmically as $\epsilon\to 0$. The speed c approaches c^* in this limit and, again, the way in which this happens is l dependent. These two properties of our model—the appearance of a dynamic selection mechanism as a limit of a qualitatively distinct solvability mechanism, and the dependence of the selected speed and shock front on the short-wavelength cutoff—so far as we know have not been seen previously in systems of this kind.

We wish to thank B. Shaw for providing Fig. 1 and also, along with J. Carlson and J. Bechhoefer, for useful discussions during the progress of this work. This research was supported by DOE Grant No. DE-FG03-84ER45108 and NSF Grant No. PHY89-04035.

[1] J. M. Carlson and J. S. Langer, Phys. Rev. Lett. **62**, 2632 (1989); Phys. Rev. A **40**, 6470 (1989).
[2] J. M. Carlson, J. S. Langer, B. Shaw, and C. Tang, Phys. Rev. A **44**, 884 (1991).
[3] R. Burridge and L. Knopoff, Bull. Seis. Soc. Am. **57**, 341 (1967).
[4] A. Kolmagorov, I. Petrovsky, and N. Piscounov, Bull. Univ. Moscow, Ser. Internat., Sec. A **1**, 1 (1937).
[5] D. G. Aronson and H. F. Weinberger, Adv. Math. **30**, 33 (1978).
[6] G. Dee and J. S. Langer, Phys. Rev. Lett. **50**, 383 (1983).
[7] E. Ben-Jacob, H. Brand, G. Dee, L. Kramer, and J. S. Langer, Physica (Amsterdam) **14D**, 348 (1985).
[8] W. van Saarloos, Phys. Rev. A **39**, 6367 (1989).
[9] There seems to be no simple analogy with previous work. Consider, for example, a nonlinear diffusion equation of the form $\partial u/\partial t=\partial^2 u/\partial s^2-\partial V/\partial u$ with $V(u)$ of the form $V(u)=-\frac{1}{2}\epsilon u^2-\frac{1}{3}u^3+\frac{1}{4}\lambda u^4$. As $\epsilon\to 0$, the metastable state at $u=(1/2\lambda)(1-\sqrt{1+4\epsilon})$ merges with the unstable state at $u=0$, and the solvability mechanism that determines the speed at which the stable state propagates into the metastable state becomes precisely consistent with the dynamic selection mechanism that governs propagation into the unstable state. The analogy is spoiled, however, by the fact that, for small enough ϵ, the selection mechanism in this system is necessarily of the nonlinear "type II" discussed in Ref. [7].